Lithosphere

Research Article

Dynamic Responses of Embedded Rock Pile Groups due to Rock Burst considering Coupled Pile-to-Pile Interaction

Xiaolin Cao [ID],[1,2] Fengxi Zhou [ID],[1] Hongbo Liu [ID],[2] and Zhitong Zhang [ID][2]

[1]*School of Civil Engineering, Lanzhou University of Technology, Lanzhou 730050, China*
[2]*School of Civil Engineering, Southeast University, Nanjing 211189, China*

Correspondence should be addressed to Xiaolin Cao; xlcao@lut.edu.cn

This note presents an analytical solution to investigate the dynamic behavior of pile groups of embedded rock due to rock burst, which takes into account the interaction between piles. The energy generated by the rock burst propagates through the soil in the form of stress waves. It is transmitted to the pile foundation through the interaction between the soil around the pile and the pile. For rock-socketed piles, the condition of pile tip fixing is considered. The horizontal dynamic response calculation model of the pile group is established, and the analytical forms of the pile group stiffness and pile group interaction factor are obtained. In addition, the effect of saturated soil parameters on the dynamic response of pile groups are discussed.

1. Introduction

Rock burst is a phenomenon of sudden failure in the open rock mass, which often occurs in deep underground mining or areas with high tectonic stress [1, 2]. Pile group foundation is often subjected to rock burst, and the load is shared by each single pile. The load distribution among individual piles is affected by the mechanical properties of each piles, pile spacing, and different configurations [3, 4]. In addition, due to the existence of pile group effect, the load distribution between the piles and along the pile body is affected, and the horizontal bearing capacity of the pile foundation is weakened [5].

The energy generated by the rock burst propagates through the soil in the form of waves. The wave propagates to the surrounding soil of the underground structure and will have an effect on the underground structure. The main research at present is the effect of rock burst on tunnels [6–12]. Based on the case of coal explosion in CSBA covering structure of 1305 working face, Mu et al. [6] found out the main controlling factors of GWS slip and established the CSBAGWS slip criterion. Through the control variable

method, Wang et al. [7] established 15 multidimensional cloud models. And it is determined that the key factors affecting the evaluation accuracy of the multidimensional cloud model are numerical features, weights, and normalization methods. Chen et al. [8] studied the effect of temperature on rock burst in deep tunnels. Some other studies [9–12] take the tunnel as the research object and analyze the influence of the soil characteristics on the rock burst on the tunnel from different emphases.

At present, there are few studies on the impact of rock burst on pile foundations. However, there are many studies on the impact of seismic waves on pile foundations [13–17]. The study of the effect of seismic waves on pile groups generally includes three steps. This is similar to the dynamic response analysis of pile groups. The first step is to obtain the resistance of the pile to the seismic waves [18–20]. The resistance includes the soil itself and the seismic wave. Based on the soil resistance obtained in the first step, the single pile analysis was performed as the second step [21–24]. The third step is to obtain the pile group stiffness through the interaction coefficient [25–30].
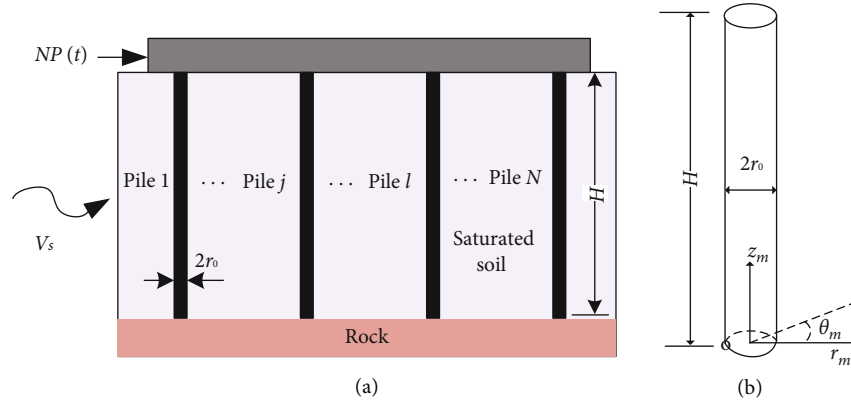
FIGURE 1: Schematic diagram of the calculation model. (a) Pile groups. (b) Single pile.

In this work, based on the research of Cao et al. [18] and considering the waves generated by the rock burst, a dynamic calculation model of the pile group is established. Afterwards, the head stiffness of pile groups is obtained by formula derivation. Finally, the dynamic interaction factor of pile groups is analyzed.

2. General Consideration

2.1. Problem Definition. In this part, based on the saturated soil resistance model given by Cao et al. [18] and considering the waves generated by the rock burst, the calculation model of the pile group in saturated soil is given as shown in Figure 1(a). We consider that the energy generated by the rock burst propagates in the soil in the form of stress waves V_s. Pile groups are embedded in saturated soil and embedded rock as a whole, and the pile head has load $NPe^{i\omega t}$, where ω is the frequency of the excitation, $i = \sqrt{-1}$. Pile numbers for N, pile length is H, pile spacing is L, and pile radius is r_0. The soil around the pile group is an isotropic, uniform, and viscoelastic saturated soil. The lame constant of the soil is a complex number. The porosity, compression coefficient, permeability coefficient, and solid-liquid coupling of saturated soil are considered in the calculation of soil resistance. The viscoelastic soil layer has complex Lame constants λ^* and G^* which remain constant with depth, Poisson's ratio υs, and mass density ρs, In the calculation process, the mth pile was first taken for analysis, as shown in Figure 1(b). Each pile and saturated soil system adopt cylindrical coordinate system (r, θ, z). The pile model is an elastic foundation beam, and the pile-soil interface slip is not considered.

2.2. Saturated Soil Resistance. In general, through literature review, it is found that analyzing the dynamic response of pile group includes three steps: the response of soil under pile load and wave action, the dynamic response of a single pile, and the dynamic response of pile groups. In this part, based on the saturated soil resistance model given by Cao et al. [18], the expression of saturated soil displacement,

stress, and resistance of saturated soil are expressed as follows:

$$
u_r = \cos(\theta) \sum_{m=0}^{\infty} \left[-B_{11m}\left(\zeta_{11m}K_0(\zeta_{11m}r) + \frac{1}{r}K_1(\zeta_{11m}r) \right) \right.
$$
$$
- B_{12m}\left(\zeta_{12m}K_0(\zeta_{12m}r) + \frac{1}{r}K_1(\zeta_{12m}r) \right)
$$
$$
\left. + B_{2m}\frac{K_1(\zeta_{2m}r)}{r} \right] \sin(a_m z),
$$

(1)

$$
u_\theta = \sin(\theta) \sum_{m=0}^{\infty} \left[-B_{11m}\frac{K_1(\zeta_{11m}r)}{r} - B_{12m}\frac{K_1(\zeta_{12m}r)}{r} \right.
$$
$$
\left. + B_{2m}\left(\zeta_{2m}K_0(\zeta_{2m}r) + \frac{1}{r}K_1(\zeta_{2m}r) \right) \right] \cos(a_m z),
$$

(2)

$$
p(z, w) = \pi\mu \sum_{m=0}^{n} R_m(\omega)W_m(\omega)
$$
$$
= \pi\mu \sum_{i=0}^{n} R_m(\omega)W_m(\omega)\sin(a_m z),
$$

(3)

where μ is the complex Lame's constants, $R_m(\omega)$ is a complex valued soil reaction factor associated with the mth soil mode:

$$
R_m(\omega) = -\frac{(\delta_{12} + \delta_{22})(\delta_{51} - \delta_{54} + \delta_{52} - \delta_{55}) + \delta_{53}(\delta_{11} + \delta_{21})}{\delta_{12}\delta_{21} - \delta_{11}\delta_{22}},
$$

(4)

where $\delta_{11} = s_{11m}K_0(s_{11m}) + K_1(s_{11m}) + \delta_0[s_{12m}K_0(s_{12m}) + K_1(s_{12m})]$, $\delta_{12} = K_1(s_{2m})$, $\delta_{21} = K_1(s_{11m}) + \delta_0 K_1(s_{12m})$, $\delta_{22} = s_{2m}K_0(s_{2m}) + K_1(s_{2m})$, $s_{11m} = r_0\zeta_{11m}$, $s_{12m} = r_0\zeta_{12m}$, $s_{2m} = r_0\zeta_{2m}$. $\delta_{51} = s_{11n}^2\eta_\sigma^2 K_1(s_{11m})$, $\delta_{52} = \eta_\sigma^2\zeta_{12m}^2 K_1(s_{12m})$, $\delta_{53} = \zeta_{2m}^2 K_1(s_{2m})$, $\delta_{54} = r_0^2(4\alpha/\mu)((1-2\nu_s)/(1-\nu_s))((\eta_s^2\zeta_{11m}^2/\kappa_2) - (a_m^2/\kappa_2) + ((\kappa_1/\kappa_2)(\omega/V_s)^2))K_1(s_{11m})$, $\delta_{55} = r_0^2(4\alpha/\mu)((1 - $

$2\nu_s)/(1-\nu_s))((\eta_s^2\zeta_{11m}^2/\kappa_2)-(a^2_m/\kappa_2)+((\kappa_1/\kappa_2)(\omega/V_s)^2))K_1$
(s_{12m}), $B_{11m}=r_0W((\delta_{12}+\delta_{22})/(\delta_{12}\delta_{21}-\delta_{11}\delta_{22}))$, $B_{12m}=$
$r_0W((\delta_{12}+\delta_{22})/(\delta_{12}\delta_{21}-\delta_{11}\delta_{22}))\delta_0$, and $B_{2m}=r_0W((\delta_{11}$
$+\delta_{21})/(\delta_{12}\delta_{21}-\delta_{11}\delta_{22}))$.

2.3. Governing Equation of the Pile. In the process of horizontal vibration of the pile group, each pile is subjected not only to the resistance of soil around the pile itself in the process of vibration but also to the resistance of soil caused by adjacent piles in the process of vibration. The pile is called source pile due to the soil resistance caused by the vibration of the pile itself $p_1(z,t)$ and considering the waves generated by the rock burst $p_2(z,t)$. The governing differential equation of the receiver pile and pile groups under the combined action of horizontal load and pile side soil resistance is

$$E_p I_p \frac{\partial^4 u_p}{\partial z^4} + m_p \frac{\partial^2 u_p}{\partial t^2} = -p_1(z,t) - p_2(z,t), \qquad (5)$$

where $E_p I_p$ is the flexural rigidity of the pile and m_p describes the pile mass per unit pile length, $p(z,t)$ is the lateral resistances of soil layers. $p_2(z,t)=U_{ff}e^{i\omega t}$, and U_{ff} is determined from the theory of one-dimensional wave propagation.

According to Equations (1) and (2), the horizontal displacement of saturated soil $u_s(r,\theta,z,\omega)$ can be expressed as

$$u_s(r,\theta,z) = \sum_{n=1}^{\infty} A_n \Gamma_n(r,\theta,\omega)\Phi_n(z), \qquad (6)$$

where A_n is the constant determined by boundary conditions and Γ_n is the displacement factor of soil defined as follows:

$$\Gamma_n(r,\theta,\omega) = \sum_{n=1}^{\infty}\left[\Gamma_{1n}(r,\omega)\cos^2(\theta)-\Gamma_{2n}(r,\omega)\sin^2(\theta)\right], \qquad (7)$$

where $\Gamma_{1n}(r,\omega)=-(\zeta_{11m}K_0(\zeta_{11m}r)+(1/r)K_1(\zeta_{11m}r))-\gamma_{11m}$
$(\zeta_{12m}K_0(\zeta_{12m}r)+(1/r)K_1(\zeta_{12m}r))+\gamma_{12m}(K_1(\zeta_{2m}r)/r)$,
$\Gamma_{2n}(r,\omega)=-(K_1\quad(\zeta_{11m}r)/r)-\gamma_{11m}(K_1(\zeta_{12m}r)/r)+\gamma_{12m}$
$(\zeta_{2m}K_0(\zeta_{2m}r)+(1/r)K_1(\zeta_{2m}r))$, $\gamma_{11m}=B_{12m}/B_{11m}$, and γ_{12m}
$=B_{2m}/B_{11m}$.

3. Model Development

3.1. Analysis of the Source Pile. We use the subscript j to represent the vibration of the source pile. Take the pile displacement as $u_{pi}(z,t)=W_i(z,\omega)e^{i\omega t}$, and substitute Equation (3) into Equation (5) to obtain the following:

$$E_p I_p \frac{\partial^4 W_j(z,\omega)}{\partial z^4} - m_p\omega^2 W_j(z,\omega)$$
$$= -\pi\mu\sum_{m=0}^{n}(1+K_S)R_m(\omega)W_{mj}(\omega)\sin(a_m z), \qquad (8)$$

where $W_j(z,\omega) = \sum_{m=0}^{\infty}W_{mj}(\omega)\cos(a_m z)$; the solution of Equation (8) can be expressed as

$$W_j(z,\omega) = A_j\sin\lambda z + B_j\cos\lambda z + C_j\sinh\lambda z$$
$$+ D_j\cosh\lambda z - \pi\mu\sum_{m=1}^{\infty}\frac{R_{mj}(\omega)W_{mj}(\omega)}{E_p I_p(a_m^4-\lambda^4)}\sin a_m z. \qquad (9)$$

Considering the complete contact of the pile-soil interface, the following equation can be obtained:

$$A_j\sin\lambda z + B_j\cos\lambda z + C_j\sinh\lambda z$$
$$+ D_j\cosh\lambda z - \pi\mu\sum_{m=1}^{\infty}\frac{R_{mj}(\omega)W_{mj}(\omega)}{E_p I_p(a_m^4-\lambda^4)}\sin a_m z$$
$$= \sum_{m=0}^{\infty}W_{mj}(\omega)\sin(a_m z), \qquad (10)$$

where $\sin\lambda z$, $\cos\lambda z$, $\sin h\lambda z$, and $\cos h\lambda z$ are expanded as Fourier sine series of parameter $W_m(\omega)$. The coefficients $W_j(z,\omega)$ can be written as follows:

$$W_j(z,\omega) = A_j\left(\sin\lambda z - \sum_{m=1}^{\infty}f_{1m}^j\sin a_m z\right)$$
$$+ B_j\left(\cos\lambda z - \sum_{m=1}^{\infty}f_{2m}^j\sin a_m z\right)$$
$$+ C_j\left(\sinh\lambda z - \sum_{m=1}^{\infty}f_{3m}^j\sin a_m z\right) \qquad (11)$$
$$+ D_j\left(\cosh\lambda z - \sum_{m=1}^{\infty}f_{4m}^j\sin a_m z\right),$$

where $\begin{bmatrix} f_{1m}^j & f_{2m}^j & f_{3m}^j & f_{4m}^j \end{bmatrix}^T = (R_{mj}(\omega)/[E_p I_{p2}(a_m^4-\lambda_2^4)/\pi\mu + R_{mj}(\omega)])\begin{bmatrix} F_{1m}^j & F_{2m}^j & F_{3m}^j & F_{4m}^j \end{bmatrix}^T$, $F_{1m}^j=(2/H)\int_0^H \sin\lambda z\sin a_m z dz = 2((\lambda H\cos\lambda H\sin a_m H)/((a_m H)^2-(\lambda H)^2))$, $F_{2m}^j=(2/H)\int_0^H\cos\lambda z\sin a_m z dz = 2((a_m H-\lambda H\sin\lambda H\sin a_m H)/((a_m H)^2-(\lambda H)^2))$, $F_{3m}^j=(2/H)\int_0^H\sinh\lambda z\sin a_m z dz = 2((\lambda H\cosh\lambda H\sin a_m H)/((a_m H)^2+(\lambda H)^2))$, and $F_{4m}^j=(2/H)\int_0^H\cosh\lambda z\sin a_m z dz = 2((a_m H+\lambda H\sinh\lambda H\sin a_m H)/((a_m H)^2+(\lambda H)^2))$.

Assume that the pile head displacement and rotation angle are W_0 and Ψ_0, respectively. We can get

$$[B]_j = [E]_j[C]_j, \qquad (12)$$

where $[C]_j=[A_j\,B_j\,C_j\,D_j]$ and matrix $[B]_j=[W_{0j}\,\Psi_{0j}\,0\,0]$. Through formula (12), we can get

$$[C]_j = [E]_j^{-1}[B]_j. \qquad (13)$$

Considering the pile end fixed, the end does not allow displacement and rotation angle, so matrix $[E]_j$ as follows:

$$[E]_j = \begin{bmatrix} \sin \lambda H - \sum_{m=1}^{\infty} f_{1m}^j & \cos \lambda H - \sum_{m=1}^{\infty} f_{2m}^j & \sinh \lambda H - \sum_{m=1}^{\infty} f_{3m}^j & \cosh \lambda H - \sum_{m=1}^{\infty} f_{4m}^j \\ \lambda \cos \lambda H & -\lambda \sin \lambda H & \lambda \cosh \lambda H & \lambda \sinh \lambda H \\ 0 & 1 & 0 & 1 \\ \lambda - \sum_{m=1}^{\infty} a_m f_{1m}^j & -\sum_{m=1}^{\infty} a_m f_{2m}^j & \lambda - \sum_{m=1}^{\infty} a_m f_{3m}^j & -\sum_{m=1}^{\infty} a_m f_{4m}^j \end{bmatrix}. \tag{14}$$

Substituting Equation (14) into Equation (13), the constant coefficients of pile displacement under the conditions of fixed pile ends can be obtained. By substituting the displacement obtained into Equation (3), the resistance expression of saturated soil on pile side can be obtained.

3.2. Analysis of the Receiver Groups. In the process of horizontal vibration of pile group, each pile is subjected not only to the resistance of soil around the pile itself in the process of vibration but also to the resistance of soil caused by adjacent piles in the process of vibration. We use coordinate transformation to study the influence of piles between piles. For any two piles in the pile group, the pile is called receiver pile due to the soil resistance caused by the vibration of the pile itself and the vibration of the neighboring pile. According to the coordinate conversion given by Luan et al. (2020) as follows:

$$r_j = \sqrt{r_l^2 + r_{lj}^2 + 2r_l r_{lj} \cos (\theta_l - \theta_{lj})}, \tag{15}$$

$$\sin \theta_j = \frac{r_{lj} \sin \theta_{lj} + r_l \sin \theta_l}{\sqrt{r_l^2 + r_{lj}^2 + 2r_l r_{lj} \cos (\theta_l - \theta_{lj})}}, \tag{16}$$

$$\cos \theta_j = \frac{r_0 \cos \theta_0 + r_l \cos \theta_l}{\sqrt{r_l^2 + r_0^2 + 2r_l r_0 \cos (\theta_l - \theta_0)}}, \tag{17}$$

where the receiver pile coordinate system is (r_l, θ_l, z_l) and the source pile coordinate system is (r_j, θ_j, z_j). r_{lj} is the distance between pile j and pile l. θ_0 is the angle between vibration direction and the line of pile j and pile l. Therefore, the soil resistance caused by the vibration of j pile to l pile is as follows:

$$p_{lj}(z, w) = -\int_0^{2\pi} \left[\sigma_r^l \left(r^l, \theta^l, z^l \right) \cos \theta' - \tau_{r\theta}^l \left(r^l, \theta^l, z^l \right) \sin \theta' \right] r_0 d\theta^l. \tag{18}$$

Combining the geometric equation and stress-strain relationship given by Cao [18] with Equation (3), we can get the soil resistance caused by the vibration of j pile to l pile from Equation (18) is as follows:

$$\begin{aligned} p_{lj}(z, w) &= \pi\mu \sum_{i=0}^{n} R_{mlj}(\omega) W_{mlj}(\omega, z) \\ &= \pi\mu \sum_{i=0}^{n} R_{mlj}(\omega) W_{mlj}(\omega) \sin (a_m z), \end{aligned} \tag{19}$$

where W_{mlj} is the displacement caused by the vibration of pile j and R_{mlj} is saturated soil reaction factor due to the vibration of pile j acting on the i pile.

According to formulas (3) and (19), the interaction factors can be obtained as follows:

$$X_{lj} = \frac{p_{lj}(z, w)}{p_l(z, w)}. \tag{20}$$

Therefore, the governing differential equation of any pile l in the pile group is as follows:

$$E_p I_p \frac{\partial^4 u_{pl}}{\partial z^4} + m_p \frac{\partial^2 u_{pl}}{\partial t^2} = -p_l(z, t) + \sum_{j=1, j\neq l}^{N} p_{lj}(z, t). \tag{21}$$

Substituting Equations (3), (11), and (21) into Equation (5), we can get

$$\begin{aligned} & E_p I_p \frac{\partial^4 W_l(z, \omega)}{\partial z^4} - m_p \omega^2 W_l(z, \omega) \\ & = -\pi\mu \sum_{m=0}^{n} \left(1 - \sum_{j=1, j\neq l}^{N} X_{lj} \right) R_{ml}(\omega) W_{ml}(\omega) \sin (a_m z). \end{aligned} \tag{22}$$
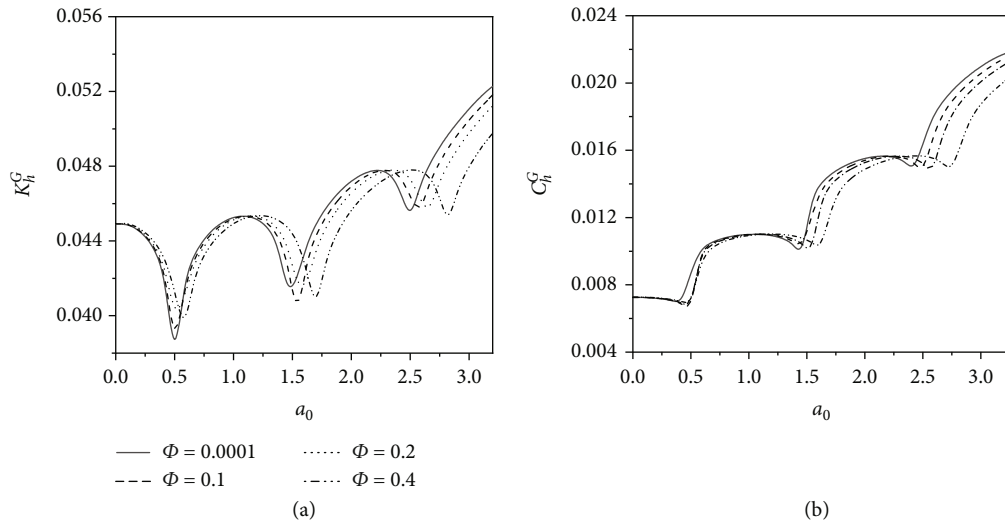
Figure 2: Variation law of pile head stiffness and damping of pile groups with porosity. (a) Real part. (b) Imaginary part.

Use the same calculation process as in Equations (9)–(11) results in the following expression for pile displacement:

$$W_l(z, \omega) = A_l \left(\sin \lambda z - \sum_{m=1}^{\infty} f_{1m}^l \sin a_m z \right)$$
$$+ B_l \left(\cos \lambda z - \sum_{m=1}^{\infty} f_{2m}^l \sin a_m z \right)$$
$$+ C_l \left(\sinh \lambda z - \sum_{m=1}^{\infty} f_{3m}^l \sin a_m z \right) \quad (23)$$
$$+ D_l \left(\cosh \lambda z - \sum_{m=1}^{\infty} f_{4m}^l \sin a_m z \right),$$

where $\left[f_{1m}^l \quad f_{2m}^l \quad f_{3m}^l \quad f_{4m}^l \right]^T = (((1 - \sum_{j=1, j\neq l}^{N} X_{lj}) R_{ml}(\omega))/[E_p I_p (a_m^4 - \lambda_2^4)/\pi\mu + R_{ml}(\omega)]) \left[F_{1m}^l \quad F_{2m}^l \quad F_{3m}^l \quad F_{4m}^l \right]^T$, $F_{1m}^l = (2/H) \int_0^H \sin \lambda z \sin a_m z\, dz = 2((\lambda H \cos \lambda H \sin a_m H)/((a_m H)^2 - (\lambda H)^2))$, $F_{2m}^l = (2/H) \int_0^H \cos \lambda z \sin a_m z\, dz =$

$2((a_m H - \lambda H \sin \lambda H \sin a_m H)/((a_m H)^2 - (\lambda H)^2))$, $F_{3m}^l = (2/H) \int_0^H \sinh \lambda z \sin a_m z\, dz = 2((\lambda H \cosh \lambda H \sin a_m H)/((a_m H)^2 + (\lambda H)^2))$, and $F_{4m}^l = (2/H) \int_0^H \cosh \lambda z \sin a_m z\, dz = 2((a_m H + \lambda H \sinh \lambda H \sin a_m H)/((a_m H)^2 + (\lambda H)^2))$.

Assume that the pile group head displacement and rotation angle are W_{0lj} and Ψ_{0lj}, respectively. We can get

$$[B]_l = [E]_l [C]_l, \quad (24)$$

where $[C]_l = [A_l \, B_l \, C_l \, D_l]$ and matrix $[B]_j = [W_{0l} \, \Psi_{0l} \, 0 \, 0]$. Through formula (24), we can get

$$[C]_l = [E]_l^{-1} [B]_l. \quad (25)$$

Considering the pile end fixed, the end does not allow displacement and rotation angle, so matrix $[E]_j$ as follows:

$$[E]_j = \begin{bmatrix} \sin \lambda H - \sum_{m=1}^{\infty} f_{1m}^l & \cos \lambda H - \sum_{m=1}^{\infty} f_{2m}^l & \sinh \lambda H - \sum_{m=1}^{\infty} f_{3m}^l & \cosh \lambda H - \sum_{m=1}^{\infty} f_{4m}^l \\ \lambda \cos \lambda H & -\lambda \sin \lambda H & \lambda \cosh \lambda H & \lambda \sinh \lambda H \\ 0 & 1 & 0 & 1 \\ \lambda - \sum_{m=1}^{\infty} a_m f_{1m}^l & -\sum_{m=1}^{\infty} a_m f_{2m}^l & \lambda - \sum_{m=1}^{\infty} a_m f_{3m}^l & -\sum_{m=1}^{\infty} a_m f_{4m}^l \end{bmatrix}. \quad (26)$$
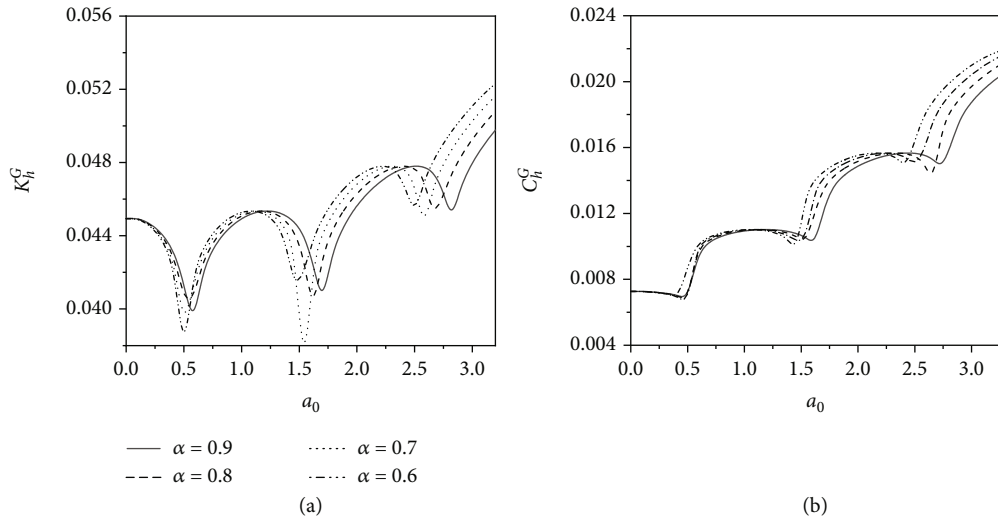
FIGURE 3: Variation law of pile head stiffness and damping of pile groups with compressibility. (a) Real part. (b) Imaginary part.
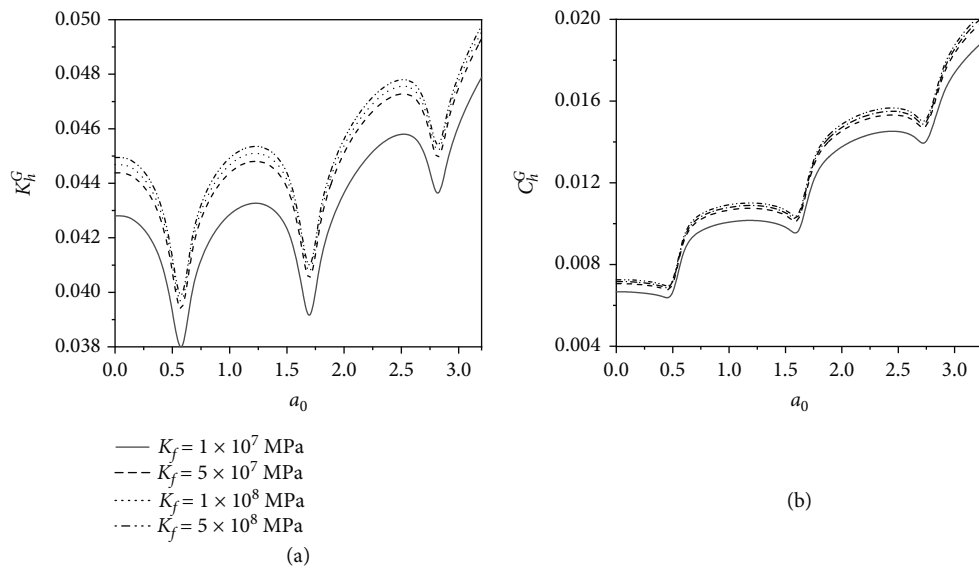

FIGURE 4: Variation law of pile head stiffness and damping of pile groups with fluid bulk modulus. (a) Real part. (b) Imaginary part.

Substituting Equation (26) into Equation (25), respectively, the constant coefficients of pile displacement under the conditions of fixed pile ends can be obtained.

3.3. Determination of Pile Group Impedance.

According to formula (22), the distribution of shear force along the pile body can be obtained as follows:

$$
\frac{S_l(z, \omega)}{E_p I} = \left(-\lambda^3 \cos \lambda z + \sum_{m=1}^{\infty} a_m^3 f_{1m} \cos a_m z \right) A_l
$$

$$
+ \left(\lambda^3 \sin \lambda z + \sum_{m=1}^{\infty} a_m^3 f_{2m} \cos a_m z \right) B_l
$$

$$
+ \left(\lambda^3 \cosh \lambda z + \sum_{m=1}^{\infty} a_m^3 f_{3m} \cos a_m z \right) C_l
$$

$$
+ \left(\lambda^3 \sinh \lambda z + \sum_{m=1}^{\infty} a_m^3 f_{4m} \cos a_m z \right) D_l.
$$

$$(27)$$

Through (25) and (26), A_l, B_l, C_l, and D_l under different pile end conditions can be obtained. Bring them into (47) to obtain the shear force at any point of the pile body. Since the force on the pile head is $NP(t)$, and the shear force on the pile head is equal to the external load
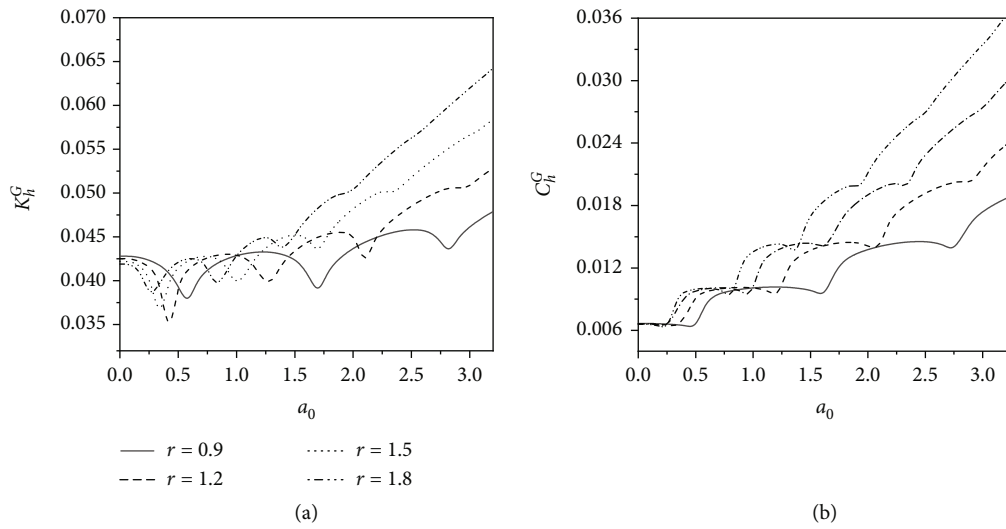
FIGURE 5: Variation law of pile head stiffness and damping of pile groups with pile spacing. (a) Real part. (b) Imaginary part.
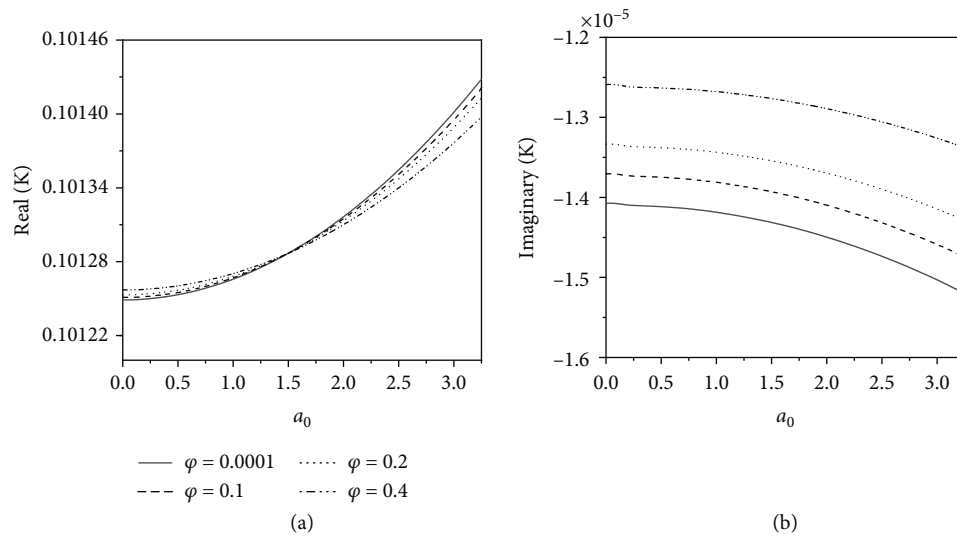

FIGURE 6: Variation of dynamic interaction factor of the pile group with porosity. (a) Real part. (b) Imaginary part.

on the pile. For the pile group with the number of piles N, the total shear force is

$$
\begin{aligned}
NPe^{i\omega t} &= \sum_{l=1}^{N} S_l(0, \omega) \\
&= E_p I \sum_{l=1}^{N} \left[\left(-\lambda^3 + \sum_{m=1}^{\infty} a_m^3 f_{1m} \right) A_l + \sum_{m=1}^{\infty} a_m^3 f_{2m} B_l \right. \\
&\quad \left. + \left(\lambda^3 + \sum_{m=1}^{\infty} a_m^3 f_{3m} \right) C_l + \sum_{m=1}^{\infty} a_m^3 f_{4m} D_l \right].
\end{aligned}
$$

(28)

For group pile foundations, the pile head is embedded in the cap as a whole. Therefore, we consider that the pile heads of the pile groups have no rotation, so $\Psi_{0lj} = 0$. The

horizontal stiffness of the pile head of the pile group is as follows:

$$
K_h^G = \frac{NPe^{i\omega t}}{U_0} = \frac{\sum_{i=1}^{N} S_i(0, \omega)}{U_0}, \tag{29}
$$

where $K_h^{\ G}$ is a complex number, the real part represents stiffness, and the imaginary part represents damping, which can be expressed as follows:

$$
K_h^G = k_h^G + i c_h^G. \tag{30}
$$

For different boundary conditions, the pile head impedance of pile groups can be obtained by Equation (30). Notably, the pile head impedance is a complex number, in which the real part and imaginary part of the pile head impedance represent the stiffness and damping of pile
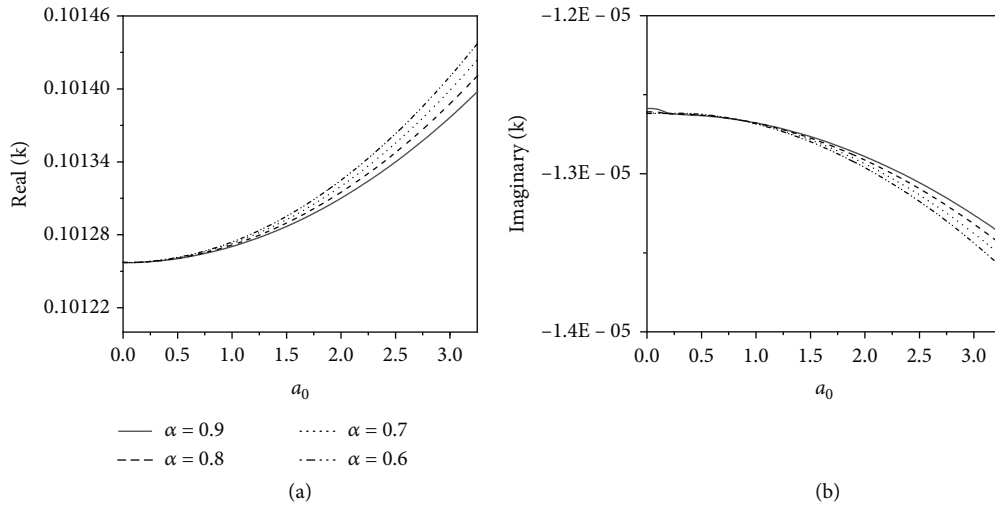
FIGURE 7: Variation of dynamic interaction factor of the pile group with compressibility. (a) Real part. (b) Imaginary part.
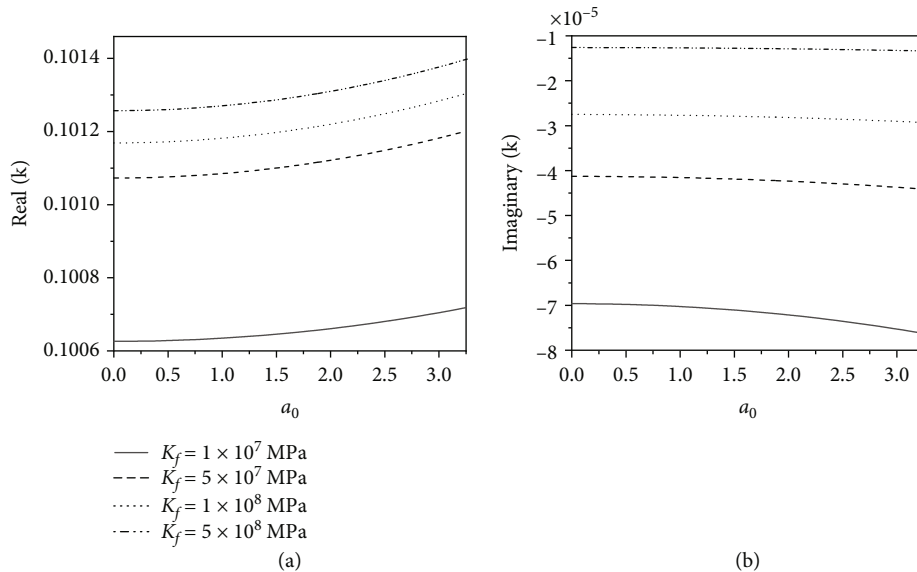

FIGURE 8: Variation of dynamic interaction factor of the pile group with fluid bulk modulus. (a) Real part. (b) Imaginary part.

groups, respectively. It depends on the parameters of the saturated soil, pile length-diameter ratio, pile spacing, and the number of pile groups.

4. Results and Discussion

In this section, numerical examples are presented to verify the correctness of the model and to analyze the influence of the saturated soil parameters on the dynamic response of the pile groups. The existing theories and experiments are used to verify the correctness of the calculation model in this paper, and the variation laws of two piles, three piles, and four piles with frequency are compared. In order to consider the effect of the interaction between the piles on the stiffness of the pile groups, a group of two piles is selected for research. Furthermore, the dynamic interac-

tion factor is used to account for pile-to-pile interactions in pile groups.

In this section, the response of the pile head stiffness and the dynamic interaction factor as a function of the normalized frequency is shown in Figures 2–8, Figure 9 for various values of the saturated soil parameters and pile spacing. Except for the analysis parameters, take pile length H = $100r_0$ m, $E_p = 27\,G_{pa}$, and $\rho_p = 2500\,kg/m^3$. To analyze the effects of resonance, the frequency is transformed to normalized frequency by $a_0 = \omega d/V_s$. The material parameters of the saturated soil are shown in Table 1.

The effects of the soil porosity, soil compression coefficient, bulk modulus of the interstitial fluid, and pile spacing on the pile head stiffness of pile groups are shown in Figures 2–5. Some general trends are observed: the stiffness of pile head of pile group is weakened, and local minimum
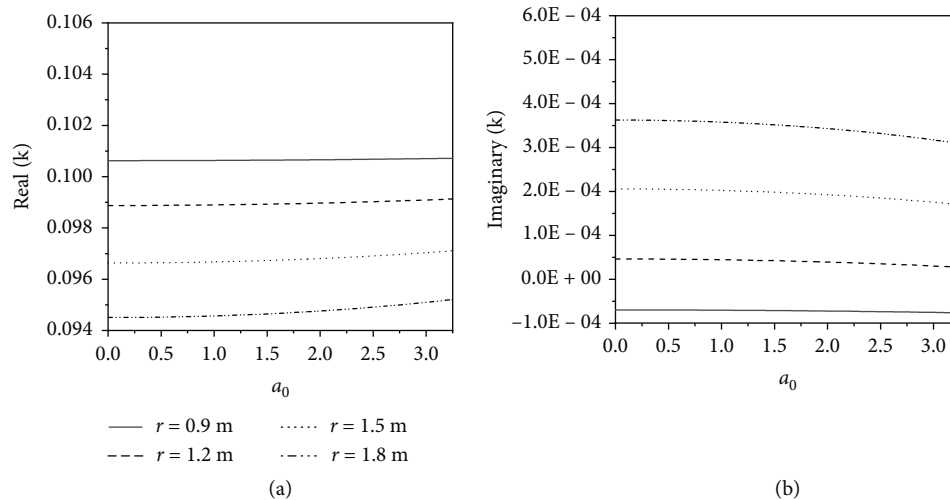
FIGURE 9: Variation of dynamic interaction factor of the pile group with pile spacing. (a) Real part. (b) Imaginary part.

TABLE 1: Numerical computer parameters for saturated porous soil [18].

Shear modulus	$G_s = 2.5$ MPa
Damping ratio	$\beta_s = 0.01$
Poisson's ratio	$v = 0.25$
Fluid density	$\rho_f = 1000$ kg/m^3
Solid density	$\rho_s = 2660$ kg/m^3
The bulk modulus of interstitial fluid	$K_f = 3.3 \times 10^7$ Pa
The bulk modulus of solid particles	$K_s = 3.7 \times 10^8$ Pa
The permeability coefficient	$k_d = 1 \times 10^{-8}$ m/s
Compression coefficient	$\alpha = 0.9$

occurs due to resonance. The pile head damping of pile groups increases due to resonance and then remains unchanged until the next resonance.

Figure 2 shows the effect of porosity on the pile head stiffness and damping of pile groups. It can be found from Figure 2(a) that with the increase of porosity, the pile head stiffness and damping decrease. This is because the increase of porosity weakens the strength of the soil, which reduces the force of the soil on the pile and reduces the stiffness of the pile head of the pile group.

Figure 3 shows the variation law of pile head stiffness and damping of pile groups with the compression coefficient. As the compression coefficient increases, the pile head stiffness and damping of the pile groups decrease. This is because the deformation of the soil under the same load increases as the compressibility increases. The stiffness of the soil is reduced, and the effect of the soil on the pile is reduced, resulting in the reduction of the stiffness of the pile head of the pile group.

Figure 4 shows the variation of pile head stiffness and damping of pile groups with liquid bulk modulus. It can be found from Figure 4 that with the increase of the liquid bulk modulus, the pile head stiffness and damping of the pile group increase. This shows that increasing the liquid bulk modulus can improve the soil properties and increase the pile head stiffness of the pile group.

Figure 5 shows the variation law of pile head stiffness and damping of pile groups with pile spacing. It can be found from Figure 5 that with the increase of the pile spacing, the pile head stiffness and damping of the pile group increase. This is because with the increase of the pile spacing, the mutual influence between the piles decreases, resulting in an increase in the stiffness of the pile head of the pile group.

The effects of the soil porosity, soil compression coefficient, bulk modulus of the interstitial fluid, and pile spacing on the dynamic interaction factor of pile groups are shown in Figures 6–9. Some general trends are observed: as the frequency increases, the real part of the dynamical interaction factor increases, while the imaginary part of the dynamical interaction factor decreases.

Figure 6 shows the variation of dynamic interaction factor of pile group with porosity. It can be found from Figure 6(a) that when $a < 1.5$, the real part of the dynamic interaction factor increases with the increase of porosity. When $a > 1.5$, the real part of the dynamic interaction factor decreases with the increase of porosity. As the porosity increases, the imaginary part of the dynamic interaction factor increases.

Figure 7 shows the variation of dynamic interaction factor of the pile group with compressibility. As the compressibility increases, the real part of the dynamic interaction factor decreases, whereas the imaginary part of the dynamic interaction factor increases.

Figure 8 shows the variation of dynamic interaction factor of the pile group with fluid bulk modulus. As the bulk modulus of the liquid increases, the real part of the dynamic interaction factor increases slightly, and the imaginary part of the dynamic interaction factor increases.

Figure 9 shows the variation of dynamic interaction factor of the pile group with pile spacing. It can be found from Figure 9 that with the increase of pile spacing, the real part of

the dynamic interaction factor decreases, while the imaginary part of the dynamic interaction factor increases.

5. Conclusions

In this paper, based on the soil resistance calculation model given by Cao et al. [18] and considering the waves generated by the rock burst, the horizontal dynamic response calculation model of the pile group is established, and the analytical solutions of the pile head stiffness and dynamic interaction factors of the pile group are obtained. The correctness of the calculation model is verified by numerical examples, and the conclusions are as follows:

(1) Through parameter analysis, it is found that the pile head stiffness and damping of pile groups increase with the decrease of porosity and compressibility of saturated soil and the increase of liquid bulk modulus and pile spacing

(2) The study found that the stiffness of pile head of the pile group is weakened and local minimum occurs due to resonance. The pile head damping of pile groups increases due to resonance and then remains unchanged until the next resonance. As the frequency increases, the real part of the dynamical interaction factor increases, while the imaginary part of the dynamical interaction factor decreases

(3) The real part of the dynamic interaction factor increases with decreasing compressibility and pile spacing of saturated soil and increasing liquid bulk modulus. The imaginary part of the dynamic interaction factor increases with the increase of compressibility coefficient, pile spacing, and liquid bulk modulus of saturated soil

Data Availability

There is no other data used in our manuscript.

Conflicts of Interest

The authors declare that they have no conflicts of interest.

Acknowledgments

References

[1] M. C. He, J. L. Miao, and J. L. Feng, "Rock burst process of limestone and its acoustic emission characteristics under true-triaxial unloading conditions," *International Journal of Rock Mechanics and Mining Sciences*, vol. 47, no. 2, pp. 286–298, 2010.

[2] Y. Yu, G. L. Feng, C. J. Xu, B. R. Chen, D. X. Geng, and B. T. Zhu, "Quantitative threshold of energy fractal dimension for immediate rock burst warning in deep tunnel: a case study," *Lithosphere*, vol. 2021, article 1699273, no. Special 4, 2022.

[3] R. Dobry and G. Gazetas, "Simple method for dynamic stiffness and damping of floating pile groups," *Geotechnique*, vol. 38, no. 4, pp. 557–574, 1988.

[4] S. Wang, L. Huang, and X. Li, "Analysis of rockburst triggered by hard rock fragmentation using a conical pick under high uniaxial stress," *Tunnelling and Underground Space Technology*, vol. 96, article 103195, 2020.

[5] G. Gazetas, K. Fan, A. Kaynia, and E. Kausel, "Dynamic interaction factors for floating pile groups," *Journal of Geotechnical Engineering*, vol. 117, no. 10, pp. 1531–1548, 1991.

[6] Z. Mu, J. Yang, G. Liu, Y. C. Zhang, J. H. Jiao, and W. Cao, "Investigation on mechanism of coal burst induced by the geological weak surface slip in coal seam bifurcation area: a case study in Zhaolou coal mine, China," *Lithosphere*, vol. 2022, no. Special 11, article 6780739, 2022.

[7] J. Wang, P. Liu, L. Ma, M. He, and H. Xiong, "A rockburst proneness evaluation method based on multidimensional cloud model improved by control variable method and rockburst database," *Lithosphere*, vol. 2021, no. Special 4, article 5354402, 2021.

[8] G. Chen, T. Li, G. Zhang, H. Yin, and H. Zhang, "Temperature effect of rock burst for hard rock in deep-buried tunnel," *Natural Hazards*, vol. 72, no. 2, pp. 915–926, 2014.

[9] Q. Jiang, X. T. Feng, T. B. Xiang, and G. S. Su, "Rockburst characteristics and numerical simulation based on a new energy index: a case study of a tunnel at 2,500 m depth," *Bulletin of engineering geology and the environment*, vol. 69, no. 3, pp. 381–388, 2010.

[10] P. Yan, Z. Zhao, W. Lu, Y. Fan, X. Chen, and Z. Shan, "Mitigation of rock burst events by blasting techniques during deep-tunnel excavation," *Engineering Geology*, vol. 188, pp. 126–136, 2015.

[11] G. L. Feng, X. T. Feng, Y. X. Xiao et al., "Characteristic microseismicity during the development process of intermittent rockburst in a deep railway tunnel," *International Journal of Rock Mechanics and Mining Sciences*, vol. 124, article 104135, 2019.

[12] G. F. Liu, Q. Jiang, G. L. Feng, D. F. Chen, B. R. Chen, and Z. N. Zhao, "Microseismicity-based method for the dynamic estimation of the potential rockburst scale during tunnel excavation," *Bulletin of Engineering Geology and the Environment*, vol. 80, no. 5, pp. 3605–3628, 2021.

[13] F. Ji and R. Y. S. Pak, "Scattering of vertically-incident P-waves by an embedded pile," *Soil Dynamics and Earthquake Engineering*, vol. 15, no. 3, pp. 211–222, 1996.

[14] A. M. Kaynia and M. Novak, "Response of pile foundations to Rayleigh waves and obliquely incident body waves," *Earthquake engineering & structural dynamics*, vol. 21, no. 4, pp. 303–318, 1992.

[15] M. Zhao, Y. Huang, P. Wang, Y. Cao, and X. Du, "An analytical solution for the dynamic response of an end-bearing pile subjected to vertical P-waves considering water-pile-soil interactions," *Soil Dynamics and Earthquake Engineering*, vol. 153, article 107126, 2021.

[16] S. M. Mamoon and P. K. Banerjee, "Response of piles and pile groups to travelling SH-waves," *Earthquake engineering & structural dynamics*, vol. 19, no. 4, pp. 597–610, 1990.

[17] J. P. Wolf and G. A. von Arx, "Horizontally travelling waves in a group of piles taking pile-soil-pile interaction into account,"

Earthquake Engineering & Structural Dynamics, vol. 10, no. 2, pp. 225–237, 1982.

[18] C. Xiaolin, D. Guoliang, G. Weiming, Z. Fengxi, and X. Jiang, "Resistance of saturated soil to a laterally vibrating pile," *Soil Dynamics and Earthquake Engineering*, vol. 141, article 106496, 2021.

[19] G. Anoyatis, G. Mylonakis, and L. Anne, "Soil reaction to lateral harmonic pile motion," *Soil Dynamics and Earthquake Engineering*, vol. 87, pp. 164–179, 2016.

[20] T. Nogami and M. J. E. E. Novak, "Resistance of soil to a horizontally vibrating pile," *Earthquake Engineering & Structural Dynamics*, vol. 5, no. 3, pp. 249–261, 2010.

[21] N. Milos, A.-E. Fakhry, and N. Toyoaki, "Dynamic soil reactions for plane strain case," *Journal of the engineering mechanics division*, vol. 104, no. 4, pp. 953–959, 1978.

[22] G. Anoyatis and L. Anne, "Dynamic pile impedances for laterally–loaded piles using improved Tajimi and Winkler formulations," *Soil Dynamics and Earthquake Engineering*, vol. 92, pp. 279–297, 2017.

[23] N. Milos and A.-E. Fakhry, "Impedance functions of piles in layered media," *Journal of the Engineering Mechanics Division*, vol. 104, no. 3, pp. 643–661, 1978.

[24] M. Novak and T. Nogami, "Soil-pile interaction in horizontal vibration," *Earthquake Engineering & Structural Dynamics*, vol. 5, no. 3, pp. 263–281, 1977.

[25] R. Sen, T. G. Davies, and P. K. Banerjee, "Dynamic analysis of piles and pile groups embedded in homogeneous soils," *Earthquake Engineering & Structural Dynamics*, vol. 13, no. 1, pp. 53–65, 1985.

[26] M. Nicos and G. Gazetas, "Dynamic pile-soil-pile interaction. Part II: lateral and seismic response," *Earthquake Engineering & Structural Dynamics*, vol. 21, no. 2, pp. 145–162, 1992.

[27] D. Francesca, C. Sandro, and L. Graziano, "A model for the 3D kinematic interaction analysis of pile groups in layered soils," *Earthquake Engineering & Structural Dynamics*, vol. 38, no. 11, pp. 1281–1305, 2009.

[28] H. Ghasemzadeh and M. Alibeikloo, "Pile–soil–pile interaction in pile groups with batter piles under dynamic loads," *Soil Dynamics and Earthquake Engineering*, vol. 31, pp. 1159–1170, 2011.

[29] M. F. Torshizi, M. Saitoh, G. M. Álamo, C. S. Goit, and L. A. Padrón, "Influence of pile radius on the pile head kinematic bending strains of end-bearing pile groups," *Soil Dynamics and Earthquake Engineering*, vol. 105, pp. 184–203, 2018.

[30] C. Xiaolin, W. Shun, G. Weiming, W. Wu, G. Dai, and F. Zhou, "Experimental and theoretical study on dynamic stiffness of single pile and pile groups in multi-layered soil," *Soil Dynamics and Earthquake Engineering*, vol. 157, article 107282, 2022.